JOURNAL OF COMPUTATIONAL PHYSICS 112, 91–101 (1994)

A New Nonstationary Boltzmann Solver in Self-Consistent Modelling of Discharge Pumped Plasmas for Excimer Lasers

D. LOFFHAGEN

Institut für Plasmaphysik, Universität Hannover, D-30167 Hannover, Germany

AND

R. WINKLER

Institut für Niedertemperatur-Plasmaphysik, D-17489 Greifswald, Germany

Received July 8, 1993; revised October 27, 1993

A self-consistent spatially homogeneous numerical model for discharge pumped excimer laser plasmas is presented with the inclusion of the nonstationary Boltzmann equation of the electrons. The nonstationary treatment of this equation (including electron–electron interaction) is based on the conventional two-term approximation and the quasi-stationary description of the anisotropic part of the velocity distribution. A detailed presentation of the new and very efficient iterative solution technique of the nonstationary electron kinetic equation is given and its integration into the complete model is described. First results of model calculations for a Ne/Xe/HCl mixture are reported in order to illustrate the new technique.

I. INTRODUCTION

Several spatially homogeneous models [1–13] have been developed to analyse preionized discharge pumped excimer laser plasmas by a self-consistent treatment of the rate equation system for the various particles and the photons, of the equation system for the electrical discharge circuit, and of the electron Boltzmann equation for the determination of the electron kinetics. Although a nonstationary treatment of the Boltzmann equation including superelastic collisions and electron–electron interaction is necessary for a strict description of the temporal evolution of the gas discharge, most models use a simplified quasi-stationary treatment of the electron kinetics, whose representation often remains very rough and unclear [14].

The recent attempts to model laser plasmas self-consistently with the inclusion of the nonstationary electron kinetics [11, 13] solve the Boltzmann equation in terms of the electron number density description based on the formulation of Rockwood [15]. Because of the matrix structure and the necessary matrix inversion in this algorithm leading to a nearly quadratic growth of computing time with the number of grid points, these models are characterized by a relatively poor energy resolution of about 100 equally or nonequally spaced grid points. Due to the pronounced structure and the sometimes very narrow action region of the electron impact cross sections of several species involved in excimer laser discharges (e.g., excitation and attachment of HCl) special care has to be taken to avoid an insufficient accuracy in collision and reaction rates resulting in incorrect predictions of the model [16].

In this paper the new self-consistent model PINBED (Program with INstationary Boltzmann solver for Excimer Discharges) for the investigation of spatially uniform gas discharges is presented. Besides the coupled system of the heavy particle kinetics, electrical circuit, and, if necessary, photon equations this model solves the nonstationary Boltzmann equation of the electrons (including superelastic collisions and electron–electron interaction) by use of a new and very efficient technique allowing for a high energy resolution with typically 1000 and more grid points. This high energy resolution becomes necessary because of the above-mentioned fine structure of several electron impact cross sections as well as in order to provide a sufficient accuracy in the treatment of the nonlinear electron–electron interaction. The nonstationary treatment of this electron kinetic equation is based on the conventional two-term approximation of the velocity distribution and the quasi-stationary (that means the neglect of the time derivative term) approximation of the anisotropic part of the distribution. The validity of both for rare-gas halide excimer laser plasmas has been shown in Ref. [14]. The high efficiency is due to the iterative use of a fast tridiagonal algorithm, and

0021-9991/94 $6.00

the high energy resolution is possible since the expense for the numerical solution of the Boltzmann equation grows only nearly linearly with the number of grid points. The model is in use for detailed investigations of a small volume coaxial discharge configuration [17] developed to check precisely the predictions of spatially homogeneous models and has proved to be excellently suitable [18, 19].

II. THEORETICAL BACKGROUND

In typical rare-gas halide discharge plasmas the strict nonstationary treatment of the electron kinetics has to include a wide spectrum of collision processes such as elastic collisions, excitation, dissociation, second kind collisions, ionization, attachment, and recombination. Furthermore, the electron–electron interaction can become an important process in comparison with the electron-heavy particle collision processes. The formulation of the nonstationary electron Boltzmann equation presented in this paper takes all of these collision processes into account. The coupling of the Boltzmann equation for the determination of the electron kinetics with the rate equation system of the various heavy particles and photons occurring in the plasma and with the electrical discharge circuit is caused by the electric field and the various densities involved in the electron-heavy particle collision processes, while the electron kinetics determines the rate coefficients for the electron-heavy particle collision processes and the plasma conductivity for the solution of the system of the electrical circuit equations and the rate equations.

Following the basic approach in Ref. [14] for solving the nonstationary electron Boltzmann equation the electron kinetics of spatially uniform excimer laser plasmas is adequately described by the temporal evolution of the isotropic part f_0 of the electron velocity distribution and of the relevant macroscopic quantities as the electron density and the different rate coefficients. This treatment is based on the two-term approximation and the quasi-stationary description of the anisotropic part of the velocity distribution. Arranging Eq. (26) of Ref. [14] with respect to terms in f_0 and its derivatives the temporal evolution of the isotropic distribution function $f_0(U, t)$ of the electrons is described by the partial differential equation, or more strictly from a mathematical point of view by the partial integro-differential equation with additional difference terms,

$$-A(U,t)\frac{\partial^2}{\partial U^2}f_0(U,t)-B(U,t)\frac{\partial}{\partial U}f_0(U,t)-C(U,t)\,f_0(U,t)+D(U)\frac{\partial}{\partial t}f_0(U,t)=G(U,t). \tag{1}$$

The coefficients A, B, C, D, and G are given by

$$\begin{aligned}
A(U,t) &= e_0^2 E(t)^2\, U\left\{\sum_j N_j(t)\left[Q_j^{\mathrm{d}}(U)+\sum_k Q_{j,k}^{\mathrm{fk}}(U)+\sum_l Q_{j,l}^{\mathrm{sk}}(U)+\sum_m Q_{j,m}^{\mathrm{i}}(U)+\sum_n Q_{j,n}^{\mathrm{a}}(U)\right]\right\}^{-1}\\
&\quad+6\left(\frac{m}{2}\right)^2\tilde{Y}(t)\left\{\frac{2}{3}\left(\int_0^U \tilde{U}^{3/2}f_0(\tilde{U},t)\,d\tilde{U}+U^{3/2}\int_U^\infty f_0(\tilde{U},t)\,d\tilde{U}\right)\right\},\\
B(U,t) &= e_0^2 E(t)^2\frac{\partial}{\partial U}\left(U\left\{\sum_j N_j(t)\left[Q_j^{\mathrm{d}}(U)+\sum_k Q_{j,k}^{\mathrm{fk}}(U)+\sum_l Q_{j,l}^{\mathrm{sk}}(U)+\sum_m Q_{j,m}^{\mathrm{i}}(U)+\sum_n Q_{j,n}^{\mathrm{a}}(U)\right]\right\}^{-1}\right)\\
&\quad+6\left(\frac{m}{2}\right)^2\tilde{Y}(t)\left\{\int_0^U \tilde{U}^{1/2}f_0(\tilde{U},t)\,d\tilde{U}+U^{1/2}\int_U^\infty f_0(\tilde{U},t)\,d\tilde{U}\right\}\\
&\quad+6U^2\sum_j\frac{m}{M_j}N_j(t)\,Q_j^{\mathrm{d}}(U),\\
C(U,t) &= \frac{\partial}{\partial U}\left\{6U^2\sum_j\frac{m}{M_j}N_j(t)\,Q_j^{\mathrm{d}}(U)\right\}\\
&\quad-3U\sum_j N_j(t)\left\{\sum_k Q_{j,k}^{\mathrm{fk}}(U)+\sum_l Q_{j,l}^{\mathrm{sk}}(U)+\sum_m Q_{j,m}^{\mathrm{i}}(U)+\sum_n Q_{j,n}^{\mathrm{a}}(U)\right\}\\
&\quad-3\left(\frac{2}{m}\right)^{-1/2}U^{1/2}\sum_q N_q(t)\,k_q(t)\\
&\quad+6\left(\frac{m}{2}\right)^2\tilde{Y}(t)\,U^{1/2}f_0(U,t),\\
D(U) &= 3\left(\frac{2}{m}\right)^{-1/2}U^{1/2},\\
G(U,t) &= 3\sum_j N_j(t)\left\{\sum_k (U+U_{j,k}^{\mathrm{fk}})\times Q_{j,k}^{\mathrm{fk}}(U+U_{j,k}^{\mathrm{fk}})\,f_0(U+U_{j,k}^{\mathrm{fk}},t)\right.\\
&\quad+\sum_l (U-U_{j,l}^{\mathrm{sk}})\,Q_{j,l}^{\mathrm{sk}}(U-U_{j,l}^{\mathrm{sk}})\times f_0(U-U_{j,l}^{\mathrm{sk}},t)\\
&\quad\left.+4\sum_m (2U+U_{j,m}^{\mathrm{i}})\times Q_{j,m}^{\mathrm{i}}(2U+U_{j,m}^{\mathrm{i}})\,f_0(2U+U_{j,m}^{\mathrm{i}},t)\right\}\\
&\quad+3\left(\frac{2}{m}\right)^{-1/2}\sum_p N_p^1(t)\,N_p^2(t)\,k_p\,U^{1/2}P_p(U).
\end{aligned} \tag{2}$$

Here t is the time, $U=mv^2/2$ is the momentary electron energy, m is the electron mass, $v=|\mathbf{v}|$ is the velocity, e_0 is the elementary charge, and $E(t)$ is the time-dependent electric field between parallel plate electrodes. $Q_j^{\mathrm{d}}(U)$, $Q_{j,k}^{\mathrm{fk}}(U)$, $Q_{j,l}^{\mathrm{sk}}(U)$, $Q_{j,m}^{\mathrm{i}}(U)$, and $Q_{j,n}^{\mathrm{a}}(U)$ denote the momentum transfer cross sections for elastic collisions and the total (that means integrated over the scattering angle) cross sections for excitation (fk—first kind collisions), for deexcitation (sk—second kind collisions), for ionization (i), and for attachment (a), respectively, related to the heavy particle component j with a time-dependent density $N_j(t)$ and a mass M_j. $\tilde{Y}(t)$ is determined by

$$\tilde{Y}(t)=\frac{1}{4\pi}\left(\frac{e_0^2}{\varepsilon_0 m}\right)^2 \ln \Lambda(t),$$
$$\Lambda(t)=\frac{8\pi}{e_0^3}\left(\frac{2}{3}\varepsilon_0^3[\bar{U}(t)]^3\frac{1}{n_e(t)}\right)^{1/2}, \tag{3}$$

where ε_0 is the vacuum permittivity. The electron density $n_e(t)$ and the mean electron energy $\bar{U}(t)$ are determined by the isotropic distribution function $f_0(U,t)$, according to

$$n_e(t)=\int_0^\infty U^{1/2} f_0(U,t)\,dU, \tag{4a}$$

$$\bar{U}(t)=\frac{1}{n_e(t)}\int_0^\infty U^{3/2} f_0(U,t)\,dU. \tag{4b}$$

$U_{j,k}^{\mathrm{fk}}$ and $U_{j,m}^{\mathrm{i}}$ denote the energy losses by excitation and ionization, $U_{j,l}^{\mathrm{sk}}$ is the energy gain by deexcitation. In accordance with [20] we assume that the kinetic energy available after each ionization event is shared equally between the two electrons. As the sum of all ionization processes only makes a small contribution to the overall collisional power dissipation and thus to the collisional response of the distribution function, the equipartition of the electron energy excess in the ionization represents a sufficient approximation. N_q and k_q are the heavy particle densities and the rate coefficients of electron loss processes due to collisions between electrons and heavy particles for which only rate coefficients are known (e.g., electron–ion recombination). Similarly k_p, N_p^1, N_p^2, and $P_p(U)$ are the rate coefficients, the heavy particle densities, and the normalized inscattering probabilities of electron production processes due to collisions between heavy particles, where for the latter the expression

$$P_p(U)=\frac{3}{4U_{\mathrm{w}}}U^{-1/2}\left[1-\left(\frac{U-U_{\mathrm{c}}}{U_{\mathrm{w}}}\right)^2\right]$$
$$\text{for}\quad U_{\mathrm{c}}-U_{\mathrm{w}}\leqslant U\leqslant U_{\mathrm{c}}+U_{\mathrm{w}}, \tag{5a}$$
$$P_p(U)=0 \qquad \text{elsewhere}$$

with the natural normalization

$$\int_0^\infty dU\, U^{1/2}P_p(U)=1 \tag{5b}$$

and with the centre U_{c} and the width U_{w} of the inscattering has been employed. For all of these processes U_{w} has been chosen so that the remaining kinetic energy is covered symmetrically by the parabolic inscattering profile around the centre U_{c}. With this approximation Penning and associative ionization as well as electron production by detachment have been included. The rate coefficients k_q often depend on the mean electron energy and consequently on time, while the rate coefficients k_p are treated as constants.

The integration of (1) over U from zero to infinity and the multiplication of (1) by U followed by the analogous integration, respectively, leads to the electron density balance

$$\frac{d}{dt}n_e(t)=\left(\frac{2}{m}\right)^{1/2}\int_0^\infty U\sum_j\sum_m N_j(t)\,Q_{j,m}^{\mathrm{i}}(U)\,f_0(U,t)\,dU$$
$$+\sum_p N_p^1(t)\,N_p^2(t)\,k_p-\left(\frac{2}{m}\right)^{1/2}$$
$$\times\int_0^\infty U\sum_j\sum_n N_j(t)\,Q_{j,n}^{\mathrm{a}}(U)\,f_0(U,t)\,dU$$
$$-\sum_q n_e(t)\,N_q(t)\,k_q(t) \tag{6}$$

and the power balance of the electrons

$$\frac{d}{dt}(n_e(t)\,\bar{U}(t))$$
$$=n_e(t)\,\bar{U}^f(t)+\sum_j\sum_l n_e(t)\,\bar{U}_{j,l}^{\mathrm{sk}}(t)$$
$$+\sum_p N_p^1(t)\,N_p^2(t)\,k_p\bar{U}_p-\sum_j n_e(t)\,\bar{U}_j^{\mathrm{el}}(t)$$
$$-\sum_j\sum_k n_e(t)\,\bar{U}_{j,k}^{\mathrm{fk}}(t)-\sum_j\sum_m n_e(t)\,\bar{U}_{j,m}^{\mathrm{i}}(t)$$
$$-\sum_j\sum_n n_e(t)\,\bar{U}_{j,n}^{\mathrm{a}}(t)-\sum_q n_e(t)\,N_q(t)\,k_q(t)\,\bar{U}(t), \tag{7}$$

respectively, where

$$\bar{U}^f(t)=b_e(t)\,e_0E(t)^2,$$
$$b_e(t)=-\frac{1}{n_e(t)}\frac{2e_0}{3m}\int_0^\infty\frac{U^{3/2}}{\nu_{im}(U,t)}\left(\frac{\partial}{\partial U}f_0(U,t)\right)dU,$$
$$\nu_{im}(U,t)=\left(\frac{2}{m}U\right)^{1/2}\sum_j N_j(t)\left(Q_j^{\mathrm{d}}(U)+\sum_k Q_{j,k}^{\mathrm{fk}}(U)\right.$$
$$\left.+\sum_l Q_{j,l}^{\mathrm{sk}}(U)+\sum_m Q_{j,m}^{\mathrm{i}}(U)+\sum_n Q_{j,n}^{\mathrm{a}}(U)\right),$$

$$\bar{U}^{sk}_{j,l}(t) = U^{sk}_{j,l}\frac{1}{n_e(t)}\left(\frac{2}{m}\right)^{1/2}\int_0^\infty N_j(t)\,UQ^{sk}_{j,l}(U)\,f_0(U,t)\,dU,$$

$$\bar{U}_p = \int_0^\infty U^{3/2}P_p(U)\,dU,$$

$$\bar{U}^{el}_j(t) = \frac{1}{n_e(t)}\left(\frac{2}{m}\right)^{1/2}\int_0^\infty N_j(t)\,2\frac{m}{M_j}U^2Q^d_j(U)\,f_0(U,t)\,dU,$$

$$\bar{U}^{fk}_{j,k}(t) = U^{fk}_{j,k}\frac{1}{n_e(t)}\left(\frac{2}{m}\right)^{1/2}\int_0^\infty N_j(t)\,UQ^{fk}_{j,k}(U)\,f_0(U,t)\,dU,$$

$$\bar{U}^{i}_{j,m}(t) = U^{i}_{j,m}\frac{1}{n_e(t)}\left(\frac{2}{m}\right)^{1/2}\int_0^\infty N_j(t)\,UQ^{i}_{j,m}(U)\,f_0(U,t)\,dU,$$

$$\bar{U}^{a}_{j,n}(t) = \frac{1}{n_e(t)}\left(\frac{2}{m}\right)^{1/2}\int_0^\infty N_j(t)\,U^2Q^{a}_{j,n}(U)\,f_0(U,t)\,dU. \tag{8}$$

$\bar{U}^f$ is the mean power input from the electric field, b_e the electron mobility, and ν_{im} the combined collision frequency for momentum dissipation. $\bar{U}^{sk}_{j,l}$ are the mean power gains by individual collision processes of second kind, $\bar{U}_p$ is the power gain by individual electron production processes described by rate coefficients, and $\bar{U}^{el}_j$, $\bar{U}^{fk}_{j,k}$, $\bar{U}^{i}_{j,m}$, and $\bar{U}^{a}_{j,n}$ are the mean power losses by individual collision processes leading to elastic scattering, excitation, ionization, and attachment.

The temporal evolution of the electron kinetic quantities is coupled to the electrical discharge circuit and the reaction kinetics of the heavy particles in the plasma by means of the electric field $E(t)$ and the various densities $N_j(t)$ of the heavy particles involved in electron collision processes. On the other hand, the electron kinetics determines the rate coefficients

$$k^p_{j,\mu}(t) = \frac{1}{n_e(t)}\left(\frac{2}{m}\right)^{1/2}\int_0^\infty UQ^p_{j,\mu}(U)\,f_0(U,t)\,dU,$$
$$p = \text{fk, sk, i, a;} \qquad \mu = k, l, m, n, \tag{9}$$

for the electron-heavy particle collision processes in the rate equation system and the plasma conductivity $\sigma = e_0 n_e(t)\,b_e(t)$ in the circuit equation system, being described by the ordinary differential equation system

$$\frac{d}{dt}\mathbf{Y} = \mathbf{F}(\mathbf{Y}) \tag{10}$$

with the initial values $\mathbf{Y}(t_0) = \mathbf{Y}_0$, where $\mathbf{Y}$ is the vector of all heavy particle densities $N(t)$ in the plasma and the time-dependent voltages $V(t)$ and currents $I(t)$ of the different branches in the electrical circuit. Neglecting the cathode fall the electric field $E(t)$ between parallel plate electrodes with a gap length d is correlated to the discharge voltage U_{Dis} according to $E(t) = U_{Dis}(t)/d$.

III. NUMERICAL APPROACH

III.1. *General Aspects*

In the numerical model presented in this paper the self-consistent treatment of discharge pumped excimer laser plasmas becomes possible by repeating up to sufficient convergence for each time step the successive solution of the coupled system of the rate equations for the heavy particles (and photons) and the electrical circuit equations on the one side and the electron Boltzmann equation on the other side. The solution of the rate and electrical circuit equations for the time step just considered yields the temporal evolution of the heavy particle densities and the electric field being necessary for the determination of the electron kinetic quantities. The solution of the Boltzmann equation of the electrons for the same time step provides then the temporal evolution of the isotropic distribution function and thus especially of the electron density, the mean electron energy, the electron mobility, and the various rate coefficients for the electron-heavy particle collision processes that couple the electron kinetics back to the heavy particle kinetics and the electrical circuit. In the following at first the separate procedures of solving for one time step (i) the nonstationary Boltzmann equation and (ii) the rate and circuit equation system are presented. Then the coupling of both procedures is explained.

An alternative way to solve the problem of the coupling of the nonstationary electron kinetics with the heavy particle kinetics and the electrical circuit has been presented in [13]. In this model the Boltzmann equation is solved by a formalism based on Rockwood [15] with a poor energy resolution of about 100 grid points.

III.2. *Nonstationary Boltzmann Equation*

The method for solving the partial differential equation (1) is a generalization of existing techniques [21–23] relevant to simpler nonstationary plasmas. Due to the inclusion of the electron–electron interaction Eq. (1) is nonlinear with the nonlinearities coming from the integral coefficients in front of the second and the first derivative of f_0 with respect to U and the quadratic term in f_0. From a physical point of view it can be expected that as long as the terms of the electron–electron interaction do not play the dominant part, the solution of Eq. (1) for each time step can be obtained by use of an iterative treatment of a corresponding linear equation.

Equation (1) is solved as an initial-boundary value problem with the time-dependence of the electric field $E(t)$ and the heavy particle densities $N_j(t)$ given for the next time interval $[t_k, t_k + \Delta t]$ just considered. Taking, additionally, the electron density balance (6) into account, the temporal behaviour of f_0 is uniquely determined in this time interval for all energies $0 \leqslant U \leqslant U_\infty$, if an appropriate initial

distribution $f_0(U, t_k)$ at the moment t_k is given and the boundary condition $f_0(U \geqslant U_\infty, t) = 0$ at a sufficiently large energy U_∞ is applied for $t_k \leqslant t \leqslant t_k + \Delta t$. A finite difference approximation for Eqs. (1) and (6) is employed using the mesh point representation

$$\begin{aligned} &U_i = (i-1)\,\Delta U, \qquad U_{n+1} = U_\infty, \qquad 1 \leqslant i \leqslant n+1; \\ &t_k = k\,\Delta t, \qquad k \geqslant 0; \\ &f_{i,k} = f_0(U_i, t_k) \end{aligned} \tag{11}$$

of an equidistant energy grid with the boundaries $U = 0$ and U_∞ and, typically, $n = 1000$ energy intervals.

The partial differential equation (1) is discretized according to the Crank–Nicolson method [24] at the points U_i, $t_{k+1/2}$ with $2 \leqslant i \leqslant n$ and $k \geqslant 0$, i.e., halfway between the known and the unknown time steps, using the finite second-order-correct difference analogues

$$\begin{aligned} f_{i,k+1/2} &= \tfrac{1}{2}(f_{i,k+1} + f_{i,k}), \\ \left(\frac{\partial}{\partial t} f\right)_{i,k+1/2} &= \frac{1}{\Delta t}(f_{i,k+1} - f_{i,k}), \\ \left(\frac{\partial}{\partial U} f\right)_{i,k+1/2} &= \frac{1}{4(\Delta U)}(f_{i+1,k+1} + f_{i+1,k} \\ &\quad - f_{i-1,k+1} - f_{i-1,k}), \\ \left(\frac{\partial^2}{\partial U^2} f\right)_{i,k+1/2} &= \frac{1}{2(\Delta U)^2}(f_{i+1,k+1} - 2f_{i,k+1} + f_{i-1,k+1} \\ &\quad + f_{i+1,k} - 2f_{i,k} + f_{i-1,k}) \end{aligned} \tag{12}$$

for f_0 and its derivatives, the analogue

$$K_{i,k+1/2} = \tfrac{1}{2}(K(U_i, t_{k+1}) + K(U_i, t_k)) \tag{13}$$

for the time-dependent coefficients $K = A$, B, C, G, and the further second-order-correct analogue

$$\begin{aligned} f_0(\beta U_i + U^{\mathrm{p}}_{j,\mu}, t_{k+1/2}) = \tfrac{1}{2}(&f_0(\beta U_i + U^{\mathrm{p}}_{j,\mu}, t_{k+1}) \\ &+ f_0(\beta U_i + U^{\mathrm{p}}_{j,\mu}, t_k)) \end{aligned} \tag{14}$$

for the various difference terms in Eq. (1) resulting from the different exciting, deexciting, and ionizing collisions. Due to the energy shift by the energy loss or gain $U^{\mathrm{p}}_{j,\mu}$ in the different inelastic collision processes the values on the right-hand side of Eq. (14) usually do not fit with the chosen energy mesh points. The representation of these values on the same energy grid (11) can be obtained with the aid of parabolic interpolations in the distribution function values $f_{i,\nu}$, $\nu = k, k+1$, which are given by

$$\begin{aligned} f_0(\beta U_i + U^{\mathrm{p}}_{j,\mu}, t_\nu) = \tfrac{1}{2}(&\alpha^{-1}_{j,\mu,p}\alpha^{0}_{j,\mu,p} f_{\beta i + n_{j,\mu,p} - 1,\nu} \\ &- 2\alpha^{+1}_{j,\mu,p}\alpha^{-1}_{j,\mu,p} f_{\beta i + n_{j,\mu,p},\nu} \\ &+ \alpha^{+1}_{j,\mu,p}\alpha^{0}_{j,\mu,p} f_{\beta i + n_{j,\mu,p} + 1,\nu}), \\ \nu = k, k+1, \end{aligned} \tag{15}$$

$$n_{j,\mu,p} = \operatorname{int}\left(\frac{U^{\mathrm{p}}_{j,\mu} + 0.5\gamma\,\Delta U}{\Delta U}\right),$$

$$\alpha^{\tau}_{j,\mu,p} = \left(\frac{U^{\mathrm{p}}_{j,\mu}}{\Delta U}\right) - n_{j,\mu,p} + \tau - \delta,$$

$$\tau = -1, 0, 1;$$

Collision process	$U^{\mathrm{p}}_{j,\mu}$	β	γ	δ
Excitation	$U^{\mathrm{fk}}_{j,k}$	1	1	0
Deexcitation	$-U^{\mathrm{sk}}_{j,l}$	1	−1	0
Ionization	$U^{\mathrm{i}}_{j,m}$	2	−1	1

The various integrals occurring in the coefficients $A(U_i, t_\nu)$ and $B(U_i, t_\nu)$, $\nu = k, k+1$, due to the electron–electron interaction are discretized for energy points U_i with odd i according to

$$\int_{U_i}^{U_\infty} f_0(\tilde{U}, t_\nu)\, d\tilde{U} = \sum_\xi \frac{\Delta U}{3}(f_{\xi,\nu} + 4f_{\xi+1,\nu} + f_{\xi+2,\nu}),$$
$$\xi = i, i+2, \ldots, n-1, \tag{16a}$$

using Simpson's rule [25] and

$$\begin{aligned} \int_0^{U_i} &\tilde{U}^{m/2} f_0(\tilde{U}, t_\nu)\, d\tilde{U} \\ &= \frac{\Delta U}{3}\left\{\frac{2}{m+2}(2\,\Delta U)^{m/2}\,[(1 + 2(\alpha-1)(\alpha-2))\, f_{1,\nu}\right. \\ &\quad - 4\alpha(\alpha-2)\, f_{2,\nu} + (1 + 2\alpha(\alpha-1))\, f_{3,\nu}] \\ &\quad \left. + \sum_\xi (U^{m/2}_\xi f_{\xi,\nu} + 4U^{m/2}_{\xi+1} f_{\xi+1,\nu} + U^{m/2}_{\xi+2} f_{\xi+2,\nu})\right\}, \\ \alpha &= 2/^{m+2}\sqrt{4}, \qquad m = 1, 3, \qquad \xi = 3, 5, \ldots, i-2, \end{aligned} \tag{16b}$$

using a modified Simpson's rule for the integration over $U^{m/2} f_0(U, t)$ with $m = 1, 3$ near the energy $U = 0$ in order to avoid larger integration errors. The modification consists of the transformation of the integral from zero to $2\,\Delta U$, according to $x = U^{(m+2)/2}$, the discretization of the transformed integral expression with the aid of Simpson's rule, and the representation of these values on the chosen energy grid (11) using parabolic interpolations. In Eq. (16b) the summation from $\xi = 3$ to $i-2$ is only to be performed for $i \geqslant 5$. The values of the integrals for the energy points U_i with even $i = 2, 4, \ldots, n$ are determined with the aid of parabolic interpolations in the integrals for energy points with odd i.

The values of the electron density and the mean electron energy at t_{k+1} in the factor (3) of the electron–electron interaction terms are parabolically extrapolated by means of the corresponding known values of the last three time steps. Due to the weak dependence of the factor (3) on the electron density and the mean electron energy the remaining inaccuracy is negligible.

Treating the various difference terms, which result from the different exciting, deexciting, and ionizing collisions and parts of the nonlinear terms of the electron–electron interaction iteratively, the complete discretization of (1) finally leads to the linear inhomogeneous equation system

$$a^{(J)}_{i,k+1/2} f^{(J+1)}_{i-1,k+1} + b^{(J)}_{i,k+1/2} f^{(J+1)}_{i,k+1} + c^{(J)}_{i,k+1/2} f^{(J+1)}_{i+1,k+1} = \delta^{(J)}_{i,k+1/2}, \qquad 2 \leqslant i \leqslant n \tag{17}$$

for $k \geqslant 0$ with

$$\begin{aligned}
\delta^{(J)}_{i,k+1/2} &= -a^{(J)}_{i,k+1/2} f_{i-1,k} + d^{(J)}_{i,k+1/2} f_{i,k} \\
&\quad - c^{(J)}_{i,k+1/2} f_{i+1,k} - (\Delta U)^2 (G^{(J)}_{i,k+1} + G_{i,k}), \\
a^{(J)}_{i,k+1/2} &= A^{(J)}_{i,k+1/2} - \frac{\Delta U}{2} B^{(J)}_{i,k+1/2}, \\
b^{(J)}_{i,k+1/2} &= -2A^{(J)}_{i,k+1/2} + (\Delta U)^2 C^{(J)}_{i,k+1/2} - 2\frac{(\Delta U)^2}{\Delta t} D_i, \\
c^{(J)}_{i,k+1/2} &= A^{(J)}_{i,k+1/2} + \frac{\Delta U}{2} B^{(J)}_{i,k+1/2}, \\
d^{(J)}_{i,k+1/2} &= 2A^{(J)}_{i,k+1/2} - (\Delta U)^2 C^{(J)}_{i,k+1/2} - 2\frac{(\Delta U)^2}{\Delta t} D_i
\end{aligned} \tag{18}$$

for the discretized distribution f_0, where the indices (J) and $(J+1)$ denote the different stages $f^{(J)}_{i,k+1}$ and $f^{(J+1)}_{i,k+1}$ of the iterative solution involved in the system (17) and its coefficients (18). In (18) thus, e.g., the quantity $A^{(J)}_{i,k+1/2}$ means

$$\begin{aligned}
A^{(J)}_{i,k+1/2} &= e_0^2 E(t_{k+1/2})^2 U_i \Bigg\{ \sum_j N_j(t_{k+1/2}) \\
&\quad \times \Bigg[Q^{\mathrm{d}}_j(U_i) + \sum_k Q^{\mathrm{ik}}_{j,k}(U_i) + \sum_l Q^{\mathrm{sk}}_{j,l}(U_i) \\
&\quad + \sum_m Q^{\mathrm{i}}_{j,m}(U_i) + \sum_n Q^{\mathrm{a}}_{j,n}(U_i) \Bigg] \Bigg\}^{-1} \\
&\quad + 6\left(\frac{m}{2}\right)^2 \tilde{Y}(t_{k+1/2}) \frac{1}{2} \Bigg\{ \frac{2}{3} \Bigg(\int_0^{U_i} \tilde{U}^{3/2} \\
&\quad \times f_0(\tilde{U}, t_k)\, d\tilde{U} + U_i^{3/2} \int_{U_i}^{\infty} f_0(\tilde{U}, t_k)\, d\tilde{U} \Bigg) \\
&\quad + \frac{2}{3} \Bigg(\int_0^{U_i} \tilde{U}^{3/2} f_0^{(J)}(\tilde{U}, t_{k+1})\, d\tilde{U} \\
&\quad + U_i^{3/2} \int_{U_i}^{\infty} f_0^{(J)}(\tilde{U}, t_{k+1})\, d\tilde{U} \Bigg) \Bigg\}.
\end{aligned}$$

The equation system (17) is completed by the electron particle balance (6), which is discretized in the same way at the points $t_{k+1/2}$, i.e., halfway between the known and the unknown time steps, again using finite second-order-correct difference analogues. Applying Simpson's rule [25] to approximate the integrals in Eq. (6) and taking into account that the electron density $n_e(t_{k+1})$ at the time t_{k+1} can be expressed by means of its discretized representation according to Eq. (4a) using the modified Simpson's rule (16b) for $i = n+1$, $v = k+1$, $m = 1$ with $\alpha = 2/4^{1/3}$, the discretization of Eq. (6) leads to the self-consistent electron particle balance

$$\sum_{i=1}^{n+1} p_{i,k+1/2} f^{(J+1)}_{i,k+1} = \delta_{1,k+1/2} \tag{19}$$

in terms of the discretized distribution f_0 with

$$\begin{aligned}
p_{i,k+1/2} &= P_i \left(1 + \frac{\Delta t}{2} \sum_q N_q(t_{k+1/2})\, k_q(t_{k+1/2}) \right) \\
&\quad + \frac{\Delta t}{2} \left(\frac{2}{m} \right)^{1/2} g_i U_i \Bigg(\sum_j \sum_n N_j(t_{k+1/2})\, Q^{\mathrm{a}}_{j,n}(U_i) \\
&\quad - \sum_j \sum_m N_j(t_{k+1/2})\, Q^{\mathrm{i}}_{j,m}(U_i) \Bigg), \\
P_1 &= \tfrac{2}{3}(2\,\Delta U)^{1/2} (1 + 2(\alpha - 1)(\alpha - 2)), \\
P_2 &= \tfrac{8}{3}(2\,\Delta U)^{1/2} \alpha(\alpha - 2), \\
P_3 &= \tfrac{2}{3}(2\,\Delta U)^{1/2} (1 + 2\alpha(\alpha - 1)) + U_3^{1/2}, \\
P_i &= 4U_i^{1/2} \qquad \text{for} \quad i = 4, 6, \ldots, n, \\
P_i &= 2U_i^{1/2} \qquad \text{for} \quad i = 5, 7, \ldots, n-1, \\
P_{n+1} &= U_{n+1}^{1/2}, \\
g_1 &= g_{n+1} = 1, \qquad g_i = 4 \qquad \text{for} \quad i = 2, 4, \ldots, n, \\
g_i &= 2 \qquad \text{for} \quad i = 3, 5, \ldots, n-1, \\
\delta_{1,k+1/2} &= \frac{3}{\Delta U} \Bigg\{ n_e(t_k) \left(1 - \frac{\Delta t}{2} \sum_q N_q(t_{k+1/2})\, k_q(t_{k+1/2}) \right) \\
&\quad + \frac{\Delta t}{2} \frac{\Delta U}{3} \left(\frac{2}{m} \right)^{1/2} \\
&\quad \times \Bigg(\sum_{i=1}^{n+1} g_i U_i \Bigg[\sum_j \sum_m N_j(t_{k+1/2})\, Q^{\mathrm{i}}_{j,m}(U_i) \\
&\quad - \sum_j \sum_n N_j(t_{k+1/2})\, Q^{\mathrm{a}}_{j,n}(U_i) \Bigg] f_{i,k} \Bigg) \\
&\quad + \Delta t \left(\sum_p N^1_p(t_{k+1/2})\, N^2_p(t_{k+1/2})\, k_p \right) \Bigg\}.
\end{aligned} \tag{20}$$

The combination of Eqs. (17) and (19), together with the difference approximation $f_{i,v}=0$, $i \geqslant n+1$, $v=k, k+1$ of the boundary condition, results in the complete equation system

$$\begin{aligned} &p_{1,k+1/2} f_{1,k+1}^{(J+1)} + p_{2,k+1/2} f_{2,k+1}^{(J+1)} + \cdots + p_{n,k+1/2} f_{n,k+1}^{(J+1)} \\ &\quad = \delta_{1,k+1/2}, \\ &a_{i,k+1/2}^{(J)} f_{i-1,k+1}^{(J+1)} + b_{i,k+1/2}^{(J)} f_{i,k+1}^{(J+1)} + c_{i,k+1/2}^{(J)} f_{i+1,k+1}^{(J+1)} \\ &\quad = \delta_{i,k+1/2}^{(J)}, \qquad 2 \leqslant i \leqslant n-1, \\ &a_{n,k+1/2}^{(J)} f_{n-1,k+1}^{(J+1)} + b_{n,k+1/2}^{(J)} f_{n,k+1}^{(J+1)} \\ &\quad = \delta_{n,k+1/2}^{(J)} \end{aligned} \tag{21}$$

for the discretized distribution function f_0 with a tridiagonal coefficient matrix and an additional first row of non-zero elements. This system (21) is solved iteratively using a fast generalized tridiagonal algorithm, which also accounts for the elimination of the first row elements.

In the first time step the iterative calculation of $f_{i,1}^{(J+1)}$ starts with the distribution $f_{i,1}^{(J)} = f_{i,0}$, $1 \leqslant i \leqslant n+1$, where $f_{i,0}$ is an appropriate initial distribution. In each further time step the iterative solution starts with the distribution function $f_{i,k+1}^{(J)} = 2f_{i,k} - f_{i,k-1}$, $1 \leqslant i \leqslant n+1$, $k \geqslant 1$, in order to accelerate the algorithm by a temporal extrapolation via the next time step, where $f_{i,k}$ and $f_{i,k-1}$ denote the convergent function values of the solution of the two preceding time steps k and $k-1$. After the determination of the coefficients $a_{i,k+1/2}^{(J)}$, $b_{i,k+1/2}^{(J)}$, $c_{i,k+1/2}^{(J)}$, and $\delta_{i,k+1/2}^{(J)}$ for $2 \leqslant i \leqslant n$, using the known distribution $f_{i,k+1}^{(J)}$ in each iteration step, the equation system (21) is solved by the above-mentioned algorithm. As necessary partial steps of this algorithm the elimination of the terms just to the right of the diagonal and the transformation of the right-hand-side terms of the system has to be made according to

$$\begin{aligned} &\beta_n = b_{n,k+1/2}^{(J)}, \\ &\beta_i = b_{i,k+1/2}^{(J)} - c_{i,k+1/2}^{(J)} \frac{a_{i+1,k+1/2}^{(J)}}{\beta_{i+1}}; \\ &\gamma_n = \frac{\delta_{n,k+1/2}^{(J)}}{\beta_n}, \\ &\gamma_i = \frac{\delta_{i,k+1/2}^{(J)} - c_{i,k+1/2}^{(J)} \gamma_{i+1}}{\beta_i}; \qquad i = (n-1), (n-2), \ldots, 2, \end{aligned} \tag{22a}$$

and the elimination of the first row elements of the matrix and the transformation of the right-hand-side of the first equation according to

$$\begin{aligned} &\varepsilon_n = p_{n,k+1/2}, \\ &\varepsilon_i = p_{i,k+1/2} - \varepsilon_{i+1} \frac{a_{i+1,k+1/2}^{(J)}}{\beta_{i+1}}; \\ &\Delta_n = \delta_{1,k+1/2}, \\ &\Delta_i = \Delta_{i+1} - \varepsilon_{i+1} \gamma_{i+1}; \qquad i = (n-1), (n-2), \ldots, 1. \end{aligned} \tag{22b}$$

Then the solution function of the $(J+1)$th iteration can be calculated from

$$\begin{aligned} &f_{1,k+1}^{(J+1)} = \frac{\Delta_1}{\varepsilon_1}, \\ &f_{i,k+1}^{(J+1)} = \gamma_i - \frac{a_{i,k+1/2}^{(J)}}{\beta_i} f_{i-1,k+1}^{(J+1)}, \qquad i = 2, 3, \ldots, n. \end{aligned} \tag{23}$$

The iterative solution process at each time step t_{k+1} is finished if the absolute deviation of the ratio of two successive distribution values from the value 1 is smaller than 10^{-5} at each energy point.

In order to guarantee a precise solution at each time step the fulfilment of the power balance of the electron component (7) is controlled. Therefore the terms on the right-hand side of Eq. (7) are calculated using the numerically obtained distribution and the time derivative of the macroscopic quantity $n_e(t)\,\bar{U}(t)$ is determined from the values of the last five time steps according to the five-point formula [25]

$$\begin{aligned} &\frac{d}{dt} n_e(t_{k+1})\,\bar{U}(t_{k+1}) \\ &\quad = \frac{1}{12\,\Delta t} (25 n_e(t_{k+1})\,\bar{U}(t_{k+1}) - 48 n_e(t_k)\,\bar{U}(t_k) \\ &\qquad + 36 n_e(t_{k-1})\,\bar{U}(t_{k-1}) - 16 n_e(t_{k-2})\,\bar{U}(t_{k-2}) \\ &\qquad + 3 n_e(t_{k-3})\,\bar{U}(t_{k-3})). \end{aligned} \tag{24}$$

By appropriate choice of Δt the power balance (7) could be satisfied with a relative error of less than 10^{-3}.

By means of the distribution function $f_0(U, t_{k+1})$ at the time t_{k+1} the electron density, the mean electron energy, the electron mobility, and the various rate coefficients for the electron-heavy particle collision processes are determined. Since the population of the isotropic distribution changes drastically during a discharge pulse, the upper energy limit U_∞ and thus the step size of the energy grid is adjusted according to the instantaneous situation during the temporal evolution.

Due to the complexity and the nonlinearity of Eq. (1) a strict analysis of the stability of the numerical solution technique presented above could not be performed. Nonetheless a stable technique for the solution of (1) could be developed.

III.3. *Rate and Electrical Circuit Equation System*

The ordinary differential equation system (10) for the reaction kinetics of the heavy particles and the electrical discharge circuit is numerically solved by means of the two-stage method of Steihaug and Wolfbrandt [26, 27]. Using a relative error tolerance of 10^{-6} during the calculation from

time t_k to $t_k + \Delta t$, $k \geq 0$, the internal step size of the second-order stable algorithm is automatically controlled by estimation of the local truncation error $\tilde{E}$ according to Ref. [27] with $\tilde{E}$ being the mean relative error.

III.4. *Description of the Model*

The basic concept of the numerical model PINBED is shown in Fig. 1. Starting at a time t_k, $k \geq 0$, with the given values of all heavy particle densities $N(t_k)$ in the plasma, the voltages $V(t_k)$, and the currents $I(t_k)$ of the different branches in the electrical circuit, and the isotropic distribution function $f_0(U, t_k)$, as well as the electron density $n_e(t_v)$, the electron mobility $b_e(t_v)$, the mean electron energy $\bar{U}(t_v)$, and the various rate coefficients $k^p_{j,\mu}(t_v)$ for the times $t_v = t_k$, $t_k - \Delta t$, $t_k - 2\,\Delta t$, the numerical model PINBED solves the two above-mentioned coupled equation systems in succession in order to determine finally the unknown values of all these quantities at the time $t_k + \Delta t$. First, the solution of system (10) involving the rate and the electrical circuit equations is performed, where the rate coefficients are used for the pure heavy particle kinetics. The electron kinetic quantities that need to be known in this time interval for this procedure are determined as first estimates by means of parabolic extrapolations with respect to time in the electron density, the electron mobility, the mean electron energy (being necessary to determine the rate coefficients $k_q(\bar{U}(t))$), and the rate coefficients (9) for the electron-heavy particle collision processes using their known values at the last three time steps. The solution of system (10) yields the heavy particle densities as well as the voltages and the currents of the different branches in the electrical circuit and thus the electric field at the time $t_k + \Delta t$. The various densities $N_j(t)$ of the heavy particles involved in electron collision processes and the electric field $E(t)$ at the times t_k and $t_k + \Delta t$ and the isotropic distribution function $f_0(U, t_k)$ are the input for the solution of the nonstationary Boltzmann equation in the same time interval. The application of the iterative technique described in Section III.2 yields then the isotropic distribution function $f_0(U, t_k + \Delta t)$ at the time $t_k + \Delta t$, which afterwards is used for the determination of the density, the mobility, and the mean energy of the electron component, and the rate coefficients (9) for the electron-heavy particle collision processes at the time $t_k + \Delta t$. To guarantee a correct temporal coupling of the rate and electrical circuit equation system (10) with the electron kinetics the extrapolated values of the electron density, the electron mobility, the mean electron energy, and the rate coefficients for the electron-heavy particle collision processes used in the solution of (10) are compared with the values at the time $t_{k+1} = t_k + \Delta t$, obtained from the solution of the nonstationary electron Boltzmann equation. If the absolute deviations of the ratios of all these quantities from the value 1 is smaller than about 10^{-4}, the solution process for this time step is finished and a next time step is treated. Otherwise the procedure just discussed is repeated for the same time step until convergence is reached, making use now of the improved electron kinetic quantities at t_{k+1} in the solution of the system (10) for the rate and the electrical circuit equations. In the practice of modelling the small volume coaxial discharge configuration described in Ref. [17] it turned out, however [18], that the solution of the electron Boltzmann equation determines the upper limit of the solution time step size Δt that usually leads to a reduction to only one cycle in the self-consistent modelling for each time step. This means that the correct coupling of the electron kinetics with the reaction kinetics of the heavy particles and the electrical circuit equations has proved to be realized in nearly one cycle of the complete system solution for each time step as long as the accuracy test of the f_0 distribution by checking the fulfilment of the nonstationary power balance of the electron component is satisfied.

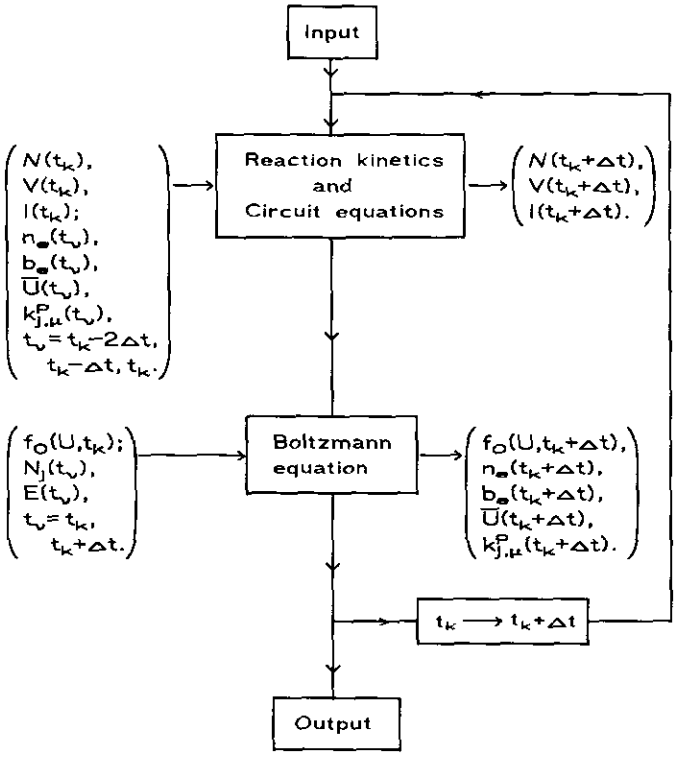

FIG. 1. Basic concept of the model PINBED.

Due to its modular structure the model can easily be changed to different homogeneous discharge configurations and (within the validity of the nonstationary electron Boltzmann equation treatment) to other gas mixtures. The flexibility of the model can be characterized by an easy adaptation to different numbers of plasma components involved in the reaction kinetics as well as to different numbers of reactions in each plasma component. A resonator equation of the photons in an optical cavity is incorporated

in the rate equation system of the model and can be activated in order to investigate laser devices.

IV. TYPICAL EXAMPLE

The calculation presented in this section was performed for a Ne/Xe/HCl mixture of 2920 mbar Ne, 75 mbar Xe, and 5 mbar HCl in the small volume coaxial discharge configuration described in Ref. [17]. For such a plasma the validity of the two-term approximation and of the quasi-stationary approximation of the anisotropic part of the velocity distribution used in the formulation of the nonstationary electron Boltzmann equation has been demonstrated in Ref. [14].

We applied an elaborate reaction kinetic model with 160 reactions in the rate equation system for 37 heavy-particle components. A list of the heavy particles included in the model and the full set of reactions are reported in [19]. The number of components relevant to the solution of the non-stationary electron Boltzmann equation amounts to 25 and the number of elastic and inelastic electron-heavy particle collision processes relevant to this equation amounts to 22 and 89, respectively. In addition to these processes being dealt with by collision cross sections further four electron loss processes by recombination and four electron production processes by detachment and ionization have been included for which only rate coefficients are known. The electrical circuit of the discharge system [17] is modelled by seven equations with the discharge parameters given in [19]. The high pressure glow discharge is generated by a fast rising (8 ns) single square pulse with a charging voltage of $U_{Ch} = 25.9$ kV and a typical duration of about 100 ns leading to a very rapid temporal evolution of the electric field, the various heavy particles, and the electron kinetic quantities. The initial distribution $f_0(U, 0)$ was taken to be Maxwellian with a mean electron energy $\bar{U}(0)$ equivalent to the gas temperature of 293 K and an electron density of $n_e(0) = 1.0 \times 10^9$ cm^{-3} was used as established by X-ray preionization. Using appropriate time step sizes such as $\Delta t = 5$ ps in the Townsend and the ignition phase, $\Delta t = 50$ ps in the quasi-steady-state phase (that means when the discharge voltage is nearly constant), and $\Delta t = 25$ ps in the recombination phase of the discharge, the iterative treatment of the difference terms due to the excitation, deexcitation, and ionization processes and of the nonlinear terms of the electron–electron interaction in the Boltzmann equation system with 1000 equations needed no more than four cycles. During the discharge the upper energy limit varies between $U_\infty = 0.8$ eV at the beginning of the calculation and about 30 eV, yielding an energy mesh size of $\Delta U \leqslant 0.03$ eV. To obtain the complete temporal evolution of the discharge with a duration of about 130 ns from the self-consistent modelling, about 10,000 time steps were used, requiring about 1 h on a vector computer Fujitsu S400/40.

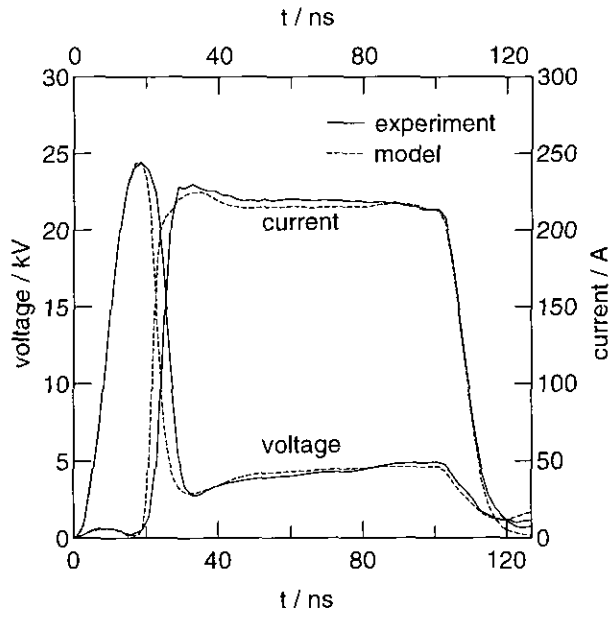

FIG. 2. Comparison of voltage and current from experiment and model.

In the following few results of this typical example will be presented. In order to illustrate the new technique the temporal course of some quantities, being relevant to the electrical circuit and the heavy particle equations as well as the electron Boltzmann equation are shown. In Fig. 2 a comparison of the model calculation with experimental results [19] is given for the temporal evolution of the voltage and the current. The quasi-steady-state voltage and current are reproduced accurately, whereas the calculated breakdown is too short by a few nanoseconds.

Figure 3 illustrates the temporal evolution of the isotropic distribution $f_0(U, t)/n_e(t)$ related to the instan-

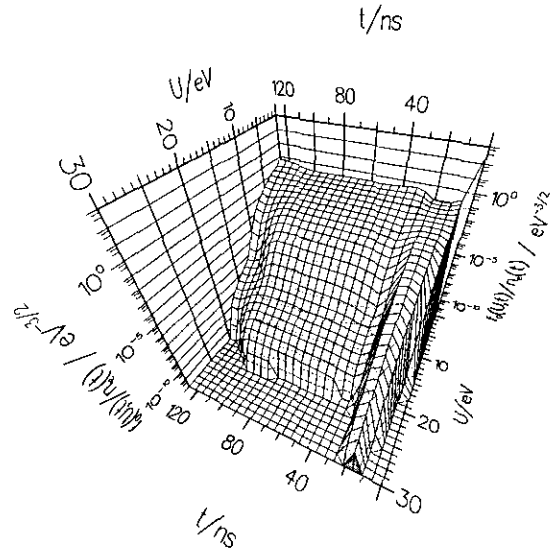

FIG. 3. Temporal evolution of the isotropic distribution $f_0(U, t)/n_e(t)$ during the discharge.

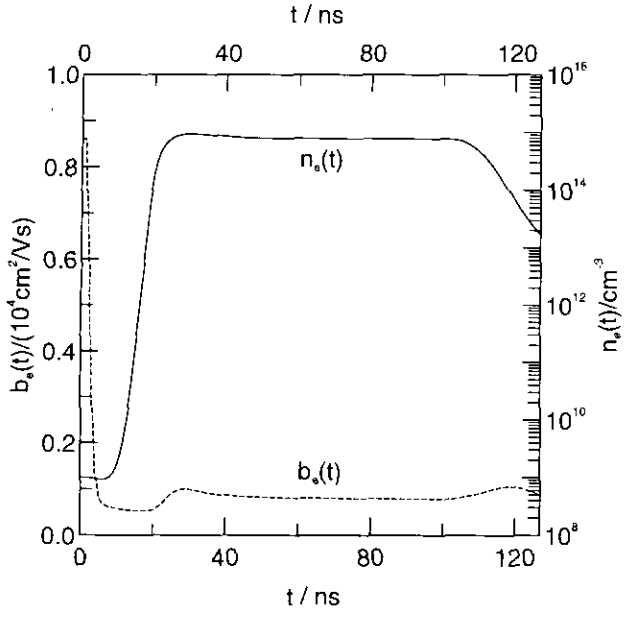

FIG. 4. Temporal evolution of the electron density and the mobility of the electrons.

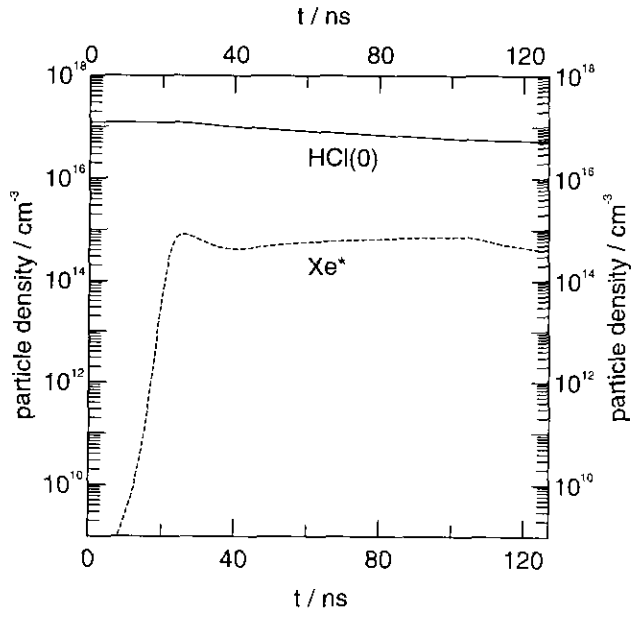

FIG. 5. Temporal evolution of the densities of HCl(0) and Xe*.

taneous electron density. In the first 6 ns of the Townsend phase of the discharge a rapid increase of the population at higher energies occurs, followed by a slower increase up to a maximum at about 18 ns. Then up to the end of the ignition phase at about $t = 40$ ns the population diminishes. In the quasi-steady-state phase the population of the distribution increases slightly, while in the recombination phase at about $t \geqslant 100$ ns a decrease of the population at higher energies is obvious. Starting from a Maxwellian distribution the isotropic distribution is subject to large structural changes during the discharge leading to pronounced non-equilibrium distributions.

The corresponding behaviour of the electron density $n_e(t)$ and of the electron mobility $b_e(t)$ is shown in Fig. 4. In connection with the rapid temporal evolution of the discharge voltage the electron density increases strongly by about six orders of magnitude, starting from its initial value due to strong ionization. In the quasi-steady-state phase of the discharge a slow decrease of the electron density occurs, followed by an exponential decrease in the recombination phase. The electron mobility, which besides the electron density determines the temporal evolution of the electrical conductivity of the discharge plasma behaves almost inversely to the overall behaviour of the isotropic distribution and thus to the behaviour of the discharge voltage or of the electric field, respectively.

Figure 5 illustrates the temporal evolution of two heavy particle densities, namely that of the mixture component HCl(0) and of the excited state Xe*. While the mixture components Ne and Xe remain almost constant throughout the whole discharge pulse a slight decrease of HCl(0), starting in the ignition phase of the discharge can be seen. The population of the excited state Xe* shows a rapid increase of the population during the Townsend and the ignition phase of the discharge, followed by comparatively slight changes of the population in the quasi-steady-state and the recombination phase.

Concerning the electron collision ionization two additional ways of the partition between the two electrons of the kinetic energy available after each collision have been included in the formalism of the Boltzmann equation.

First, the assumption of the equipartition of the electron energy excess in the collision is replaced by the treatment of the collisional ionization given by Oxenius and Simonneau [28]. Making the assumption that after the ionization collision all allowed energies and all directions of the two outgoing electrons are equally probable, these authors obtain a representation of the collision term involving only the total cross section for collisional ionization.

Following Rockwood [15] we assume, second, that one of the two electrons occurring after each ionization event enters the distribution with zero energy, while the other electron is treated as any other electron undergoing electron number conservative inelastic collisions with the energy loss equal to the ionization potential.

Model calculations using the latter treatment of the collisional ionization show a little overpopulation of the electron distribution function at energies smaller than 0.3 eV and a slightly enlarged discrepancy in the breakdown compared to the experiment. Apart from that the model calculations using different descriptions of the ionization yield nearly the same results. This emphasizes the above-

mentioned small contribution of the sum of all ionization processes to the overall collisional power dissipation and thus to the collisional response of the distribution.

V. CONCLUSIONS

A new self-consistent spatially homogeneous model of pulsed glow discharges has been developed. The main improvement of this model PINBED consists in the solution of the complex electron Boltzmann equation including superelastic collisions and electron–electron interaction by means of a new and very efficient technique allowing for a high energy resolution with 1000 and more energy grid points. The nonstationary treatment of this equation is based on the two-term approximation of the velocity distribution and on a quasi-stationary description of the anisotropic part of the distribution.

First results of the self-consistent model for a high pressure glow discharge in Ne/Xe/HCl show good agreement with experimental measurements. A more detailed comparison with experimental results for the small volume discharge configuration presented in Ref. [17] over a wide range of parameter variations and a description of the reaction kinetic model is published in [19].

The model calculation reported in this paper has been performed for a particular gas mixture in a special discharge configuration. However, in the above-mentioned validity limits of the nonstationary Boltzmann equation treatment the numerical model is applicable to a wide variety of similar problems, as excimer discharges in other mixtures, and can immediately be generalized to different discharge configurations of excimer lasers. Furthermore, this efficient technique can easily be adapted to the investigation of other pronounced nonstationary and nearly spatially homogeneous discharge plasmas occurring in various applications.

ACKNOWLEDGMENTS

We thank W. Bötticher and J. Wilhelm for administrative help. This paper is part of the Ph.D. thesis of D. Loffhagen who gratefully acknowledges the continuous interest of F. Demmig. This work was in part sponsored by the BMFT R&D projects 13N5722/3 and 13N5406/9.

REFERENCES

1. A. E. Greene and Ch. A. Brau, *IEEE J. QE*-**14**, 951 (1978).
2. T. H. Johnson, L. J. Palumbo, and A. M. Hunter, *IEEE J. QE*-**15**, 289 (1979).
3. M. Maeda, A. Takahashi, T. Mizunami, and Y. Miyazoe, *Jpn. J. Appl. Phys.* **21**, 1161 (1982).
4. H. Hokazono, K. Midorikawa, M. Obara, and T. Fujioka, *J. Appl. Phys.* **56**, 680 (1984).
5. A. V. Dem'yanov, V. S. Egorov, I. V. Kochetov, A. P. Narpatovich, A. A. Pastor, N. P. Penkin, P. Y. Serdobintsev, and N. N. Shubin, *Sov. J. Quant. Electron.* **16**, 817 (1986).
6. M. Ohwa and M. Obara, *J. Appl. Phys.* **59**, 32 (1986).
7. T. Hammer, "Untersuchungen zur Reaktionskinetik gasentladungsgepumpter XeCl*-Laser mittels hochzeitaufgelöster absorptionsspectroskopischer Messungen von Xe*-Teilchenzahldichten," Ph.D. thesis, Universität Hannover, 1987; G. Stielow, "Verifikation eines einfachen Modells einer XeCl*-Laserentladung durch Messung von Strom, Spannung und Laseremission," Ph.D. thesis, Universität Hannover, 1987.
8. G. Stielow, Th. Hammer, and W. Bötticher, *Appl. Phys. B* **47**, 333 (1988); Th. Hammer and W. Bötticher, *Appl. Phys. B* **48**, 73 (1989).
9. V. Mihkelsoo, P. Miidla, V. Peet, A. Sherman, R. Sorkina, E. Tamme, and A. Treshchalov, *J. Phys. B* **22**, 1489 (1989).
10. M. Ohwa and M. J. Kushner, *J. Appl. Phys.* **65**, 4138 (1989).
11. S. Longo, C. Gorse, and M. Capitelli, *IEEE Trans. Plasma Sci.* **19**, 379 (1991); C. Gorse, M. Capitelli, and A. Dipace, *J. Appl. Phys.* **67**, 1118 (1991).
12. U. Krause and J. Kleinschmidt, *Contrib. Plasma Phys.* **31**, 101 (1991).
13. E. Estocq and J. Bretagne, "A Self-consistent Model for X-ray Preionized XeCl Laser," in *Contributed Papers, XX ICPIG, Barga, Italy, 1991*, edited by V. Palleschi and M. Vaselli, pp. 1188; E. Estocq, G. Delouya, and J. Bretagne, *Appl. Phys. B* **56**, 209 (1993).
14. R. Winkler and M. W. Wuttke, *Appl. Phys. B* **54**, 1 (1992).
15. S. D. Rockwood, *Phys. Rev. A* **8**, 2348 (1973).
16. T. Hammer, in *Proceedings, SPIE 1278, Excimer Lasers and Applications II, The Hague, The Netherlands, 1990*, edited by T. Letardi, p. 119.
17. W. Bötticher, H. Lück, St. Niesner, and A. Schwabedissen, *Appl. Phys. B* **54**, 295 (1992).
18. D. Backhaus, Ph.D. thesis, Universität Hannover, 1992; (D. Backhaus = D. Loffhagen).
19. H. Lück, D. Loffhagen, and W. Bötticher, *Appl. Phys. B* **58**, 123 (1994).
20. H. Margenau, *Phys. Rev.* **73**, 297 (1948).
21. J. Wilhelm and R. Winkler, *J. Phys. Coll. C 7, Suppl. 7* **40**, 251 (1979).
22. R. Winkler and J. Wilhelm, *Comput. Phys. Commun.* **20**, 113 (1980).
23. R. Winkler and J. Wilhelm, "Electron Kinetics in Collision Dominated RF Plasmas," in *Invited Papers, XIX ICPIG, Belgrade, Yugoslavia, 1989*, edited by V. J. Žigman, p. 108.
24. D. U. von Rosenberg, *Methods for the Numerical Solution of Partial Differential Equations* (Am. Elsevier, New York, 1969).
25. M. Abramowitz and I. A. Stegun, *Handbook of Mathematical Functions* (Dover, New York, 1970).
26. T. Steihaug and A. Wolfbrandt, *Math. Comput.* **33**, 521 (1979).
27. R. E. Scraton, *Int. J. Comput. Math.* **9**, 81 (1981).
28. J. Oxenius and E. Simonneau, *J. Quant. Spectrosc. Radiat. Transfer* **44**, 351 (1990).